

*GYMNOMITRION BLANKAE* (MARCHANTIOPHYTA), A NEW SPECIES  
FROM YUNNAN PROVINCE, CHINA

*GYMNOMITRION BLANKAE* (MARCHANTIOPHYTA) – НОВЫЙ ВИД  
ИЗ КИТАЙСКОЙ ПРОВИНЦИИ ЮНЬНАНЬ

ALEXEY D. ПОТЕМКИН<sup>1</sup>, ANNA A. VILNET<sup>2</sup> & YURIY S. MAMONTOV<sup>2,3</sup>

АЛЕКСЕЙ Д. ПОТЕМКИН<sup>1</sup>, АННА А. ВИЛЬНЕТ<sup>2</sup>, ЮРИЙ С. МАМОНТОВ<sup>2,3</sup>

Abstract

*Gymnomitrium blankae* sp. nov. arisen from the *G. revolutum* collection from Yunnan Province, China, differs from European *G. revolutum*, described from the Tyrolean Alps, in morphology, ecology and distribution, namely in the cinnamon to rusty color (vs. fuscous, blackish or olive fuscous), leaves with sinus mostly γ-like and reflexed backwards (vs. sinus usually V- or U-like and not or slightly reflexed backwards), apiculate leaf lobes with rolled apiculi (vs. rounded to blunt and hardly apiculate lobes with not or slightly rolled apiculi), smooth leaf and stem surfaces (vs. leaf surface bearing dome-shaped projections above the cell wall intersections and stem surface ± papillose), stem with ± thinned outer walls of flattened outer cortical cells forming the indistinct hyalodermis (vs. stem with thickened outer walls of often not flattened outer cortical cells, not forming hyalodermis), occurrence on base-rich (vs. acid) rocks, the Sino-Himalayan vs. European distribution as well as in ITS2 nrDNA and trnL-F cpDNA nucleotide sequences. The DNA data obtained for specimens of *G. revolutum* from North and South Tyrol (Austria and Italy, respectively), and from adjacent territories of Switzerland represent the first molecular accessions for this species based on the collection from the type locality (Tyrolean Alps) and neighboring territories. *Gymnomitrium revolutum* from the type locality is illustrated for the first time.

Резюме

Новый для науки вид *Gymnomitrium blankae*, выявленный в коллекции *G. revolutum* из китайской провинции Юньнань, отличается от европейского *G. revolutum*, описанного из Тироляских Альп, морфологией, экологией и распространением, а именно коричневой до ржавой, а не бурой, черноватой или оливково-бурой окраской; листьями большей частью с γ-образной вырезкой сомкнутой при основании и отогнутой назад, а не преимущественно V-или U-образной вырезкой, чаще не отогнутой назад при основании; заостренными верхушками лопастей листьев с трубкообразно свернутым заострением, а не закругленными до коротко заостренных верхушками листьев, как правило, без трубкообразно свернутого заострения; гладкой, а не папиллозной поверхностью листа и стебля; ± утонченными, а не утолщенными внешними стенками уплощенных наружных клеток коры, образующих (не образующих) нечеткий гиалодермис; встречаемостью на основных, а не на кислых породах; сино-гималайским, а не европейским распространением, а также нуклеотидными последовательностями ITS2 яДНК и trnL-F хпДНК. Для *G. revolutum* впервые получены нуклеотидные последовательности для образцов из Северного и Южного Тироля (из Австрии и Италии соответственно), а также с прилегающих территорий Швейцарии, которые являются первыми молекулярными данными о виде из типового местонахождения (Тироляских Альп) и с прилегающих территорий. Впервые приводятся фотографии *G. revolutum*, основанные на материале из типового местонахождения.

KEYWORDS: *Apomarsupella*, Gymnomitriaceae, convergence, taxonomy, integrative approach.

INTRODUCTION

The genus *Gymnomitrium* Corda appears to be a suite of taxonomic surprises caused by the still obscure variability of known species and criteria for their differentiation. This equally concerns both small- and large-sized species. Recent descriptions and reappraisal of well-known

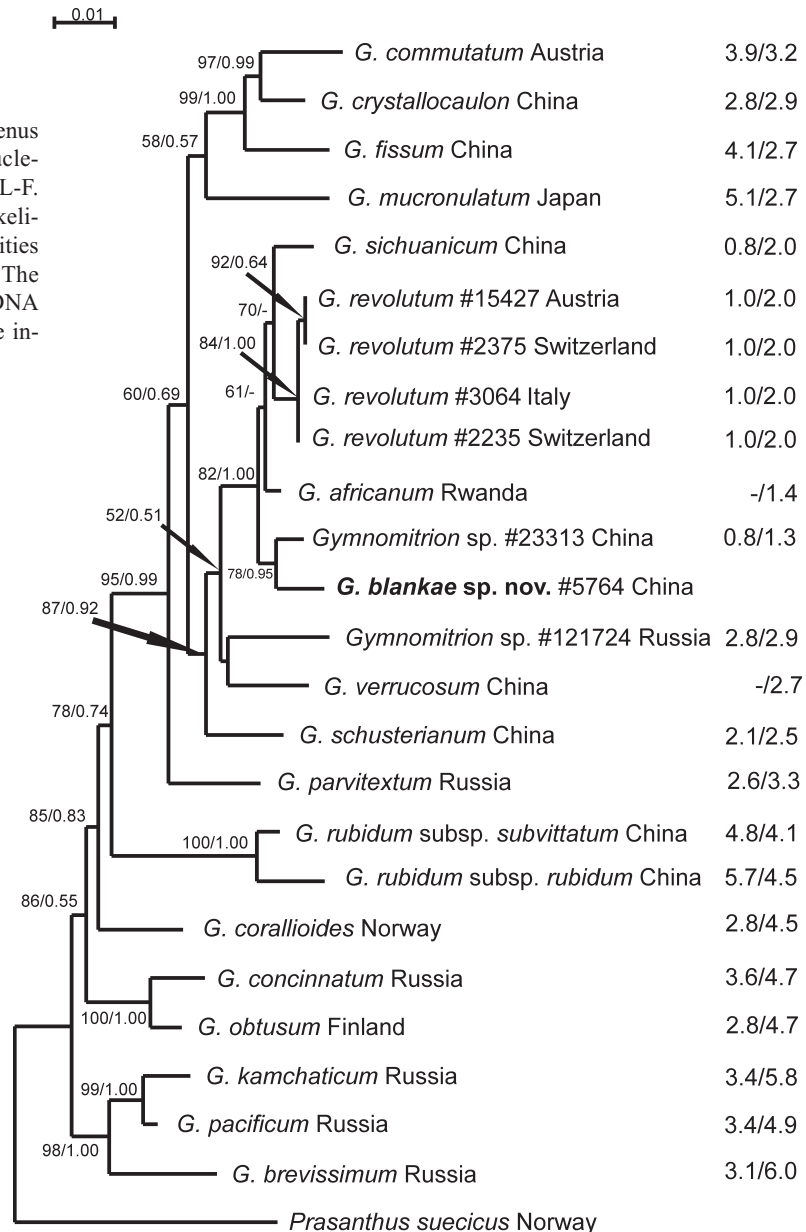
species (Potemkin *et al.*, 2017; Mamontov *et al.*, 2018, 2019; Konstantinova *et al.*, 2021; Bakalin *et al.*, 2022) are remarkable. During the last five years, another five species were added to the 33 species recognized by Söderström *et al.* (2016): *G. fissum* Mamontov & Potemkin, *G. parvitextum* (Steph.) Mamontov *et al.*, *G. kamchaticum*

1 – Komarov Botanical Institute, Russian Academy of Sciences, Professor Popov Str. 2, St. Petersburg, 197376 Russia; e-mail: Potemkin\_alexey@binran.ru, ORCID 0000-0003-4420-1704

2 – Polar-Alpine Botanical Garden-Institute of, Kola Science Centre of the Russian Academy of Sciences, Kirovsk, 184256 Russia; e-mail: anya\_v@list.ru; ORCID 0000-0001-7779-2593

3 – Tsitsin Main Botanical Garden, Russian Academy of Sciences, Botanicheskaja 4, Moscow, 127276 Russia; e-mail: yur-mamontov@yandex.ru, ORCID 0000-0003-3851-0738

Fig. 1. The ML phylogram for the genus *Gymnomitrium* based on combined nucleotide sequences dataset of ITS1-2+trnL-F. Bootstrap supports from maximum likelihood and Bayesian posterior probabilities more than 50% (0.50) are indicated. The values of *p*-distances (%) for trnL-F cpDNA between *G. blankae* and other taxa are indicated at the right.



Mamontov et al., *G. schusterianum* Konstant. et al., and *G. sichuanicum* Bakalin & Vilnet. All were described from Asia: Sino-Himalaya, the Russian Far East and Japan.

The ongoing study of Himalayan collections of *Gymnomitrium* has allowed a comparison of the specimens formerly attributed to *G. revolutum* (Nees) H. Philib. ( $\equiv$  *Marsupella revoluta* (Nees) Dumort., *Apomarsupella revoluta* (Nees) R.M. Schust.). A molecular phylogenetic analysis of *Gymnomitrium* specimen B. Shaw 5764 from Yunnan Province, China was first made by Shaw et al. (2015), where it was found in the former *Apomarsupella*-clade and cited as *G. revolutum*. Even after several subsequent phylogenetic studies with descriptions of new *Gymnomitrium* species from Himalaya (Konstantinova et al., 2021, Bakalin et al., 2022) the question of the correct identification of this specimen remained, which compelled us to sequence additional accessions of *G. revolutum* to clarify its morphological plasticity and geographical distribution.

The specimens from Austria and Italy collected in the Northern and Southern Tyrolean Alps were chosen as representative from the type locality (Nees, 1836). They have much in common with two specimens from Switzerland and distinct from Chinese one that is described below as new to science, *G. blankae*.

#### MATERIALS AND METHODS

##### Morphological study

We followed Buch's (1928) approach for measuring the complex leaves of *Scapania* and for defining the leaf length from the middle of the insertion to the level of the lobe tips. The photomicrographs were obtained using two microscopes equipped with digital cameras, a Leitz Wetzlar Orthoplan light microscope and an MSP-2 dissection microscope. To better illustrate three-dimensional objects, photomicrographs were combined from several optical sections using the stack-

ing software HeliconFocus 8. For images of dry plants of *Gymnomitrium blankae* and images of *G. revolutum* from the South Tyrolean Alps, an Olympus Stylus Tough TG-5 camera was used. SEM images were taken using a JEOL JSM-6390LA scanning electron microscope.

In addition to the below-cited type of *G. blankae*, the following specimens of *G. revolutum* from the type locality (Tyrolean Alps), Switzerland, and Norway were used for morphological study:

Norway, Sør-Trøndelag: Dovre, “Kongvold, reg. betul. fuktig klippvægg mot norr” (Atl. Fl. Eur. UTM grid NQ 2, 62°20' N, 09°40' E), 25.VII.1882, Lindberg (MHA – Hepaticae Exsiccatae S.O. Lindberii, No. 361. *Marsupella revoluta*); Switzerland, Grisons, Films, La Palas, between Segnesshütter and Segnespass, siliceous rock, nutrient rich (Xantoria), 6.IX.2019 Kiebacher 2235 (LE B-0026405 duplicate ex Herb. T. Kiebacher); Switzerland, Grisons, Falera, Crap Masegn, rock outcrop on exposed ridge, N-exposed inclined face, green schist, 7.IX.2019 Kiebacher 2275 (LE B-0026406 duplicate ex Herb. T. Kiebacher); [Austria] Tyrolia centralis, in irrigate ad latera septentrionem et occidentem versus dependentia montis Hanneburger prope Volders in Valle Oeni inf.; solo schistoso; 2500<sup>m</sup> s. m., Leithe (LE B-0026404 – Flora Exsiccata Austro-Hungarica, No. 740. *Marsupella revoluta*); Tyrolia septentrionalis, circa lacum “Blende-See” ad Kühtai; 2300<sup>m</sup> s. m., Loika (LE B-0026403 – Flora Exsiccata Austro-Hungarica, No. 1532. *Sarcoscyphus revolutus* Nees); [Northern] Tyrol, Tuxer Alpen, Grat zwischen Steinernem Lamm und Kahlwandspitze, ca. 2500 m.s.m., N-facing siliceous rocks, 17.VIII.2013, Köckinger 15427 (LE B-0026401 – duplicate ex Herb. H. Köckinger); Italy, South Tyrol, Ratschings, along path between Mt. Ratschinger Kreuz and Mt. Hohe Ferse, 2501 m a.s.l., 46.88161° N, 11.26218° E, S-facing rock outcrops at ridge, 9.X.2021, Kiebacher 3064 (LE B-0026402 – duplicate ex Herb. T. Kiebacher).

#### Taxa sampling for molecular analyses

The specimen determined as *Gymnomitrium revolutum* from China (*B. Shaw* 5764) and four European specimens (Italy, *T. Kiebacher* 3064; Austria, *H. Köckinger* 15427; Switzerland, *T. Kiebacher* 2235 and 2375) became a focus of molecular phylogenetic estimation. The ingroup also includes 18 previously published specimens of the genus *Gymnomitrium* (*Shaw et al.*, 2015, *Konstantinova et al.*, 2021, *Bakalin et al.*, 2022) and *Prasanthus suecicus* (Gottsche) Lindb. as an outgroup taxon (Appendix 1). The ITS1-2 nrDNA and *trnL*-F cpDNA were used as molecular markers, two specimens from *Shaw et al.* (2015) presented by *trnL*-F data only. Additionally, ITS2 and *trnL*-F for *Gymnomitrium* sp. *J. Shevock* 23313 from China was firstly obtained here, as well the *trnL*-F nucleotide sequence for specimen previously published as *Gymnomitrium revolutum* from Trans-Baikal Territory, Russia (*Konstantinova et al.*, 2021) was firstly obtained here. The treatment of the last specimen became questionable in the course of this study and needs future investigation.

#### DNA isolation, PCR amplification and DNA sequencing

DNA from dried *Gymnomitrium* plants was extracted with DNeasy Plant Mini Kit (Qiagen, Germany) and ITS1-2 and *trnL*-F regions were amplified and sequencing with primers suggested by White *et al.* (1990) and Taberlet *et al.* (1991) respectively. PCR was carried out in 20 µl volumes with the following amplification cycles: 3 min at 94 °C, 30 cycles (30 s 94 °C, 40 s 56 °C, 60 s 72 °C) and 2 min of final extension time at 72 °C. Amplified fragments were visualized on 1% agarose TAE gels by EthBr staining, purified using the Cleanup Mini Kit (Evrogen, Russia), and used as a template in sequencing reactions with the ABI Prism BigDye Terminator Cycle Sequencing Ready Reaction Kit (Applied Biosystems, USA) following the standard protocol provided for 3100 Avant Genetic Analyzer (Applied Biosystems, USA).

#### Phylogenetic analysis

Newly obtained nucleotide sequence data and both datasets (ITS1-2 and *trnL*-F) were produced in the program BioEdit 7.0.1 (Hall, 1999). There is no incongruence between each alignment as suggested by preliminary phylogenetic estimation, thus both dataset were combined for subsequent analyses. All positions of alignment were taken into account, absent data were coded as missing.

The phylogenetic reconstructions provided by the maximum likelihood method (ML) with IQ-TREE (Nguyen *et al.*, 2015) and the Bayesian approach (BA) with MrBayes v. 3.2.1 (Ronquist *et al.*, 2012). The ML analysis included the search of the best fit evolutionary model of nucleotide substitutions with incorporated option ModelFinder (Kalyaanamoorthy *et al.*, 2017) and ultrafast bootstrapping (Hoang *et al.*, 2018) with 1000 replicates. The TN+G was selected as the best fit evolutionary model with four rate categories of gamma distribution to evaluate the rate of heterogeneity among sites. For the Bayesian analysis ITS1-2 and *trnL*-F partitions was separately assigned the GTR+I+G model as recommended by program's creators; gamma distributions were approximated with four rate categories. Two independent runs of the Metropolis-coupled MCMC were used to sample parameter values in proportion to their posterior probability. Each run included three heated chains and one unheated chain, and the two starting trees were chosen randomly. The number of generations was one million, and trees were saved every 100 generation. Average standard deviation of split frequencies between two runs was 0.004731. The 2500 (25%) trees were discarded in each run, and 15000 trees from both runs were sampled after burning. Bayesian posterior probabilities were calculated from trees sampled after burn-in.

The infrageneric variability was estimated for ITS2 and *trnL*-F due to presence these data for tested specimen *B. Shaw* 5764. It was calculated as the average pairwise *p*-distances in Mega 11 (Tamura *et al.*, 2021) using the pairwise deletion option for counting gaps.



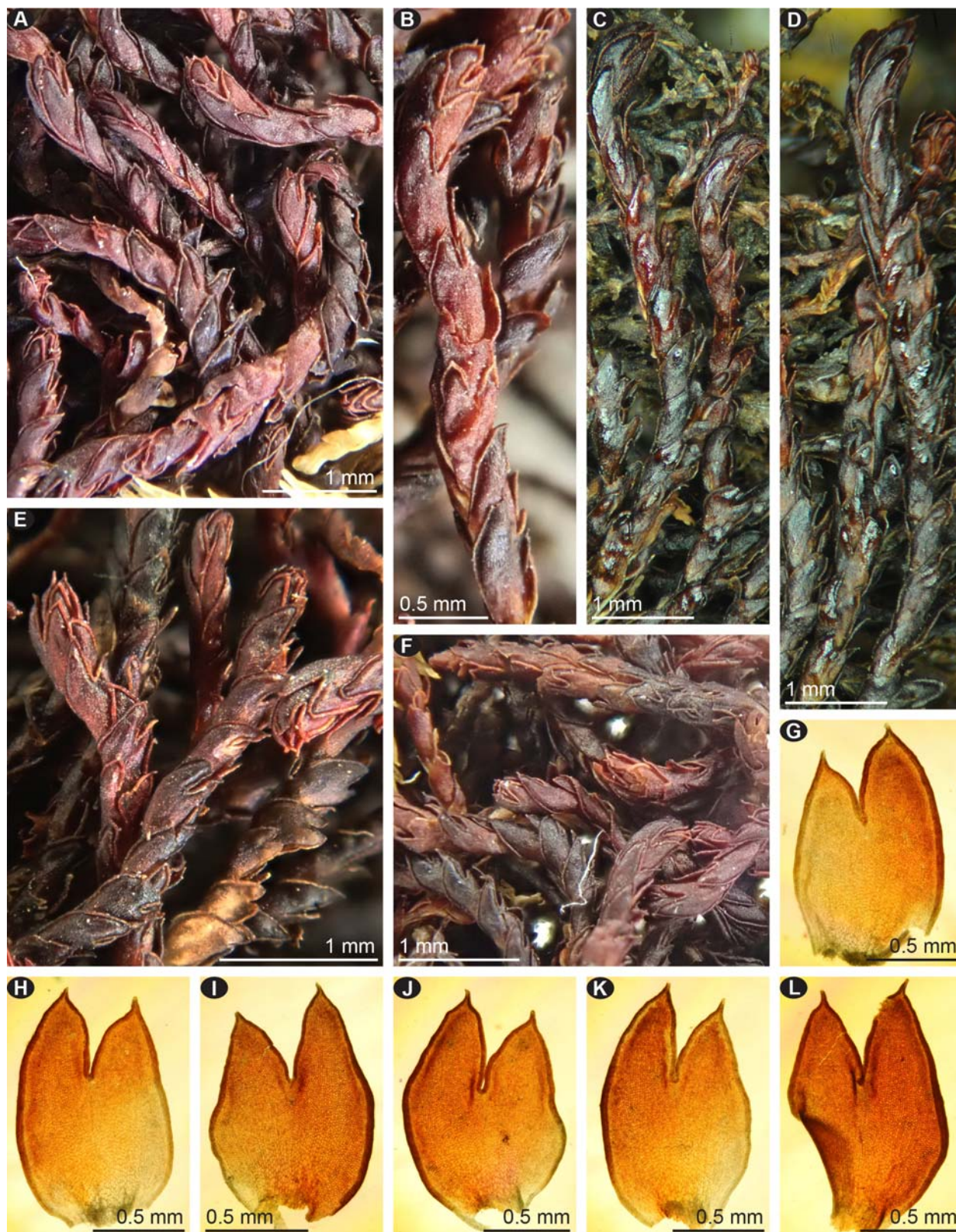


Fig. 2. *Gymnomitrium blankae* (from B. Shaw 5764, LE B-0026804, isotype). A–F: dry habit; G–I, K, L: leaves (outer side); J: male bract.

#### RESULTS

Twelve newly obtained nucleotide sequences from seven specimens were deposited into GenBank. The combined ITS1-2+*trnL*-F alignment for 21 specimens consists of

1337 sites, of which 869 belong to ITS1-2 and 468 to *trnL*-F. The ML calculation resulted in a single tree with the arithmetic means of Log likelihood -4043.754, in the BA analysis for both sampled runs were -3981.79 and -3981.89,



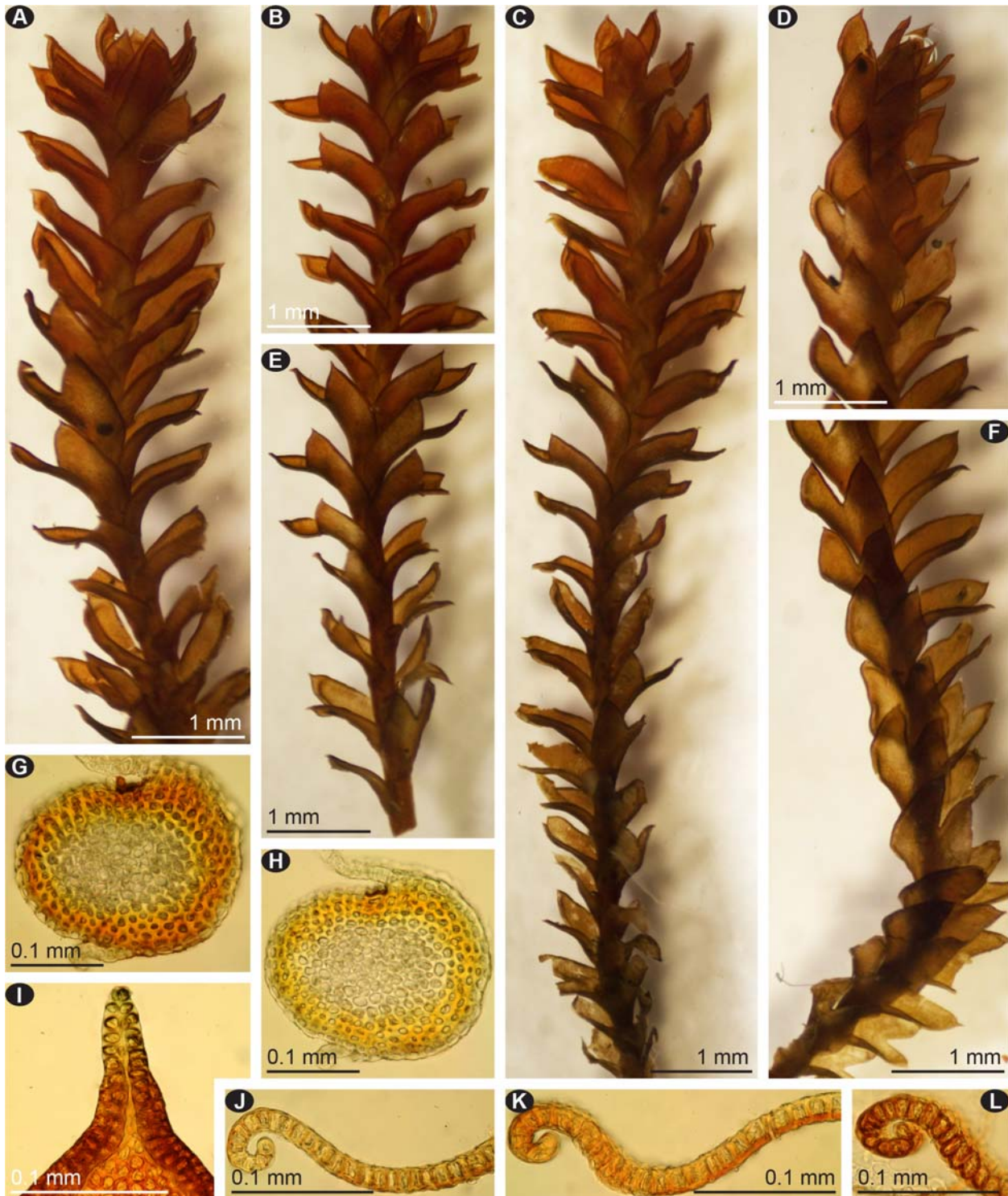


Fig. 3. *Gymnomitrium blankae* (from: B. Shaw 5764, LE B-0026804, isotype). A, C: male shoots, dorsal aspect; B, E: upper and lower parts of the same sterile shoot, respectively (dorsal aspect); D, F: upper and lower parts of the same male shoot, respectively (lateral aspect); G, H: stem cross sections; I: acuminate leaf lobe apex; J–L: parts of leaf cross sections.

respectively. The resulted trees possess a common topology, thus Fig. 1 presents a ML tree with indication of bootstrap support (BS) values from ML analyses and Bayesian posterior probabilities (PP) from BA.

The phylogenetic affinities among species in the genus *Gymnomitrium* kept stability in course of previous results (Konstantinova *et al.*, 2021, Bakalin *et al.*, 2022).

Four European specimens of *G. revolutum* composed a clade with supports BS=84, BA=1.00 (or 84/1.00) in a sister relation to the recently described *G. sichuanicum* (70/-). *Gymnomitrium revolutum* specimen B. Shaw 5764 from China was placed in affinity to other Chinese specimen of *Gymnomitrium* sp. J. Schevock 23313 (78/0.95), but still kept its position in relation to *G. sichuanicum*



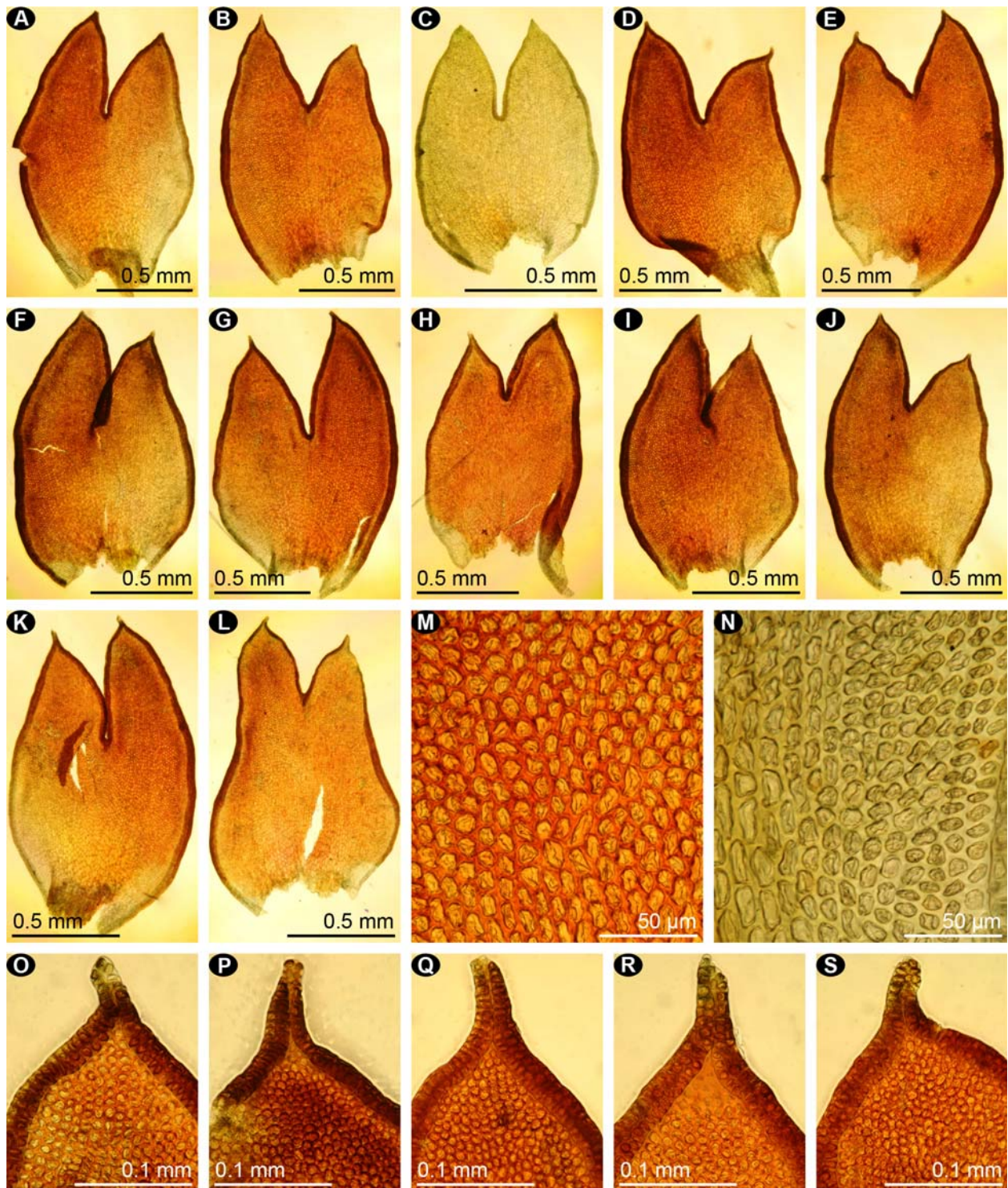


Fig. 4. *Gymnomitrion blankae* (from *B. Shaw* 5764, LE B-0026804, isotype). A–E, G, H, J, K: leaves (outer surface); F, I, L: male bracts (outer surface); M: mid-leaf cells; N: cells of the leaf base near margin; O–S: acuminate leaf lobe apices (outer surface).

(here plus clade of European specimens of *G. revolutum*) and *G. africanum* (82/1.00) (cf. Konstantinova *et al.*, 2021, Bakalin *et al.*, 2022). Thus, the accessions named as *G. revolutum* from Europe and China do not reveal close affinity to each other. The value of *p*-distance between nucleotide sequences of *B. Shaw* 5764 and European specimens achieved 1% in ITS2 and 2% in *trnL-F*,

between *B. Shaw* 5764 and the nearest related Chinese specimen *J. Schevock* 23313 – 0.8% in ITS2 and 1.3% in *trnL-F* (Fig. 1), which fits well in the frame of divergence between species in the genus *Gymnomitrion* (Bakalin *et al.*, 2022). The European specimens of *G. revolutum* vary in 0–0.2% in ITS2 and are stable in *trnL-F*. The absence of close phylogenetic affinity and significant level



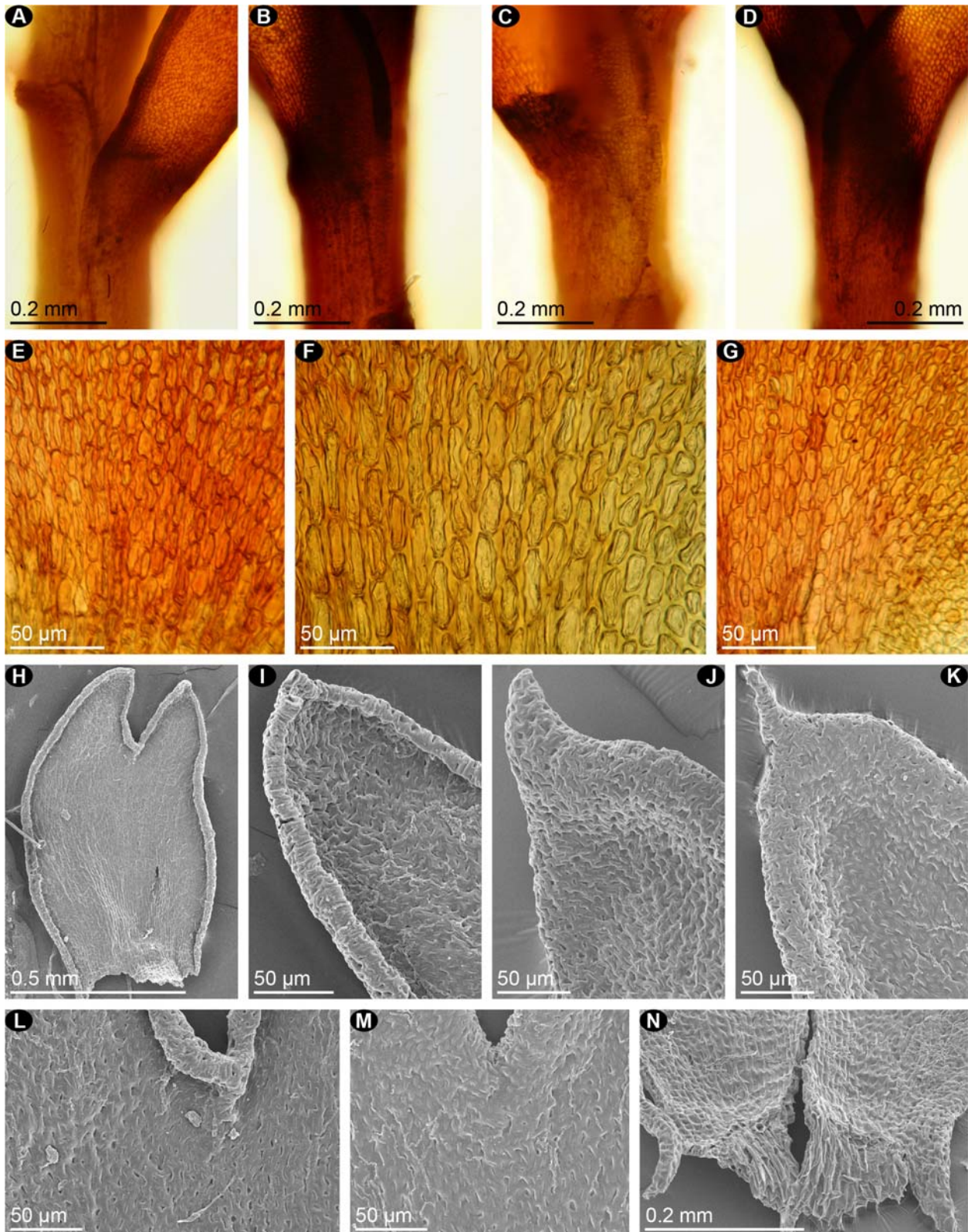


Fig. 5. *Gymnomitrium blankae* (from B. Shaw 5764, LE B-0026804, isotype (A–G), DUKE-180581 – holotype (H–N)). A–D: shoot fragments showing leaf insertion and decurrent leaf bases (A: dorsal aspect, B–D: vental aspect). E–G: basal leaf cells; H–K: SEM photographs (H, I, L: outer surface; J, K, M, N: inner surface), H: leaf; I–K: leaf lobes; L, M: parts of leaves showing sinus base; N: leaf base.



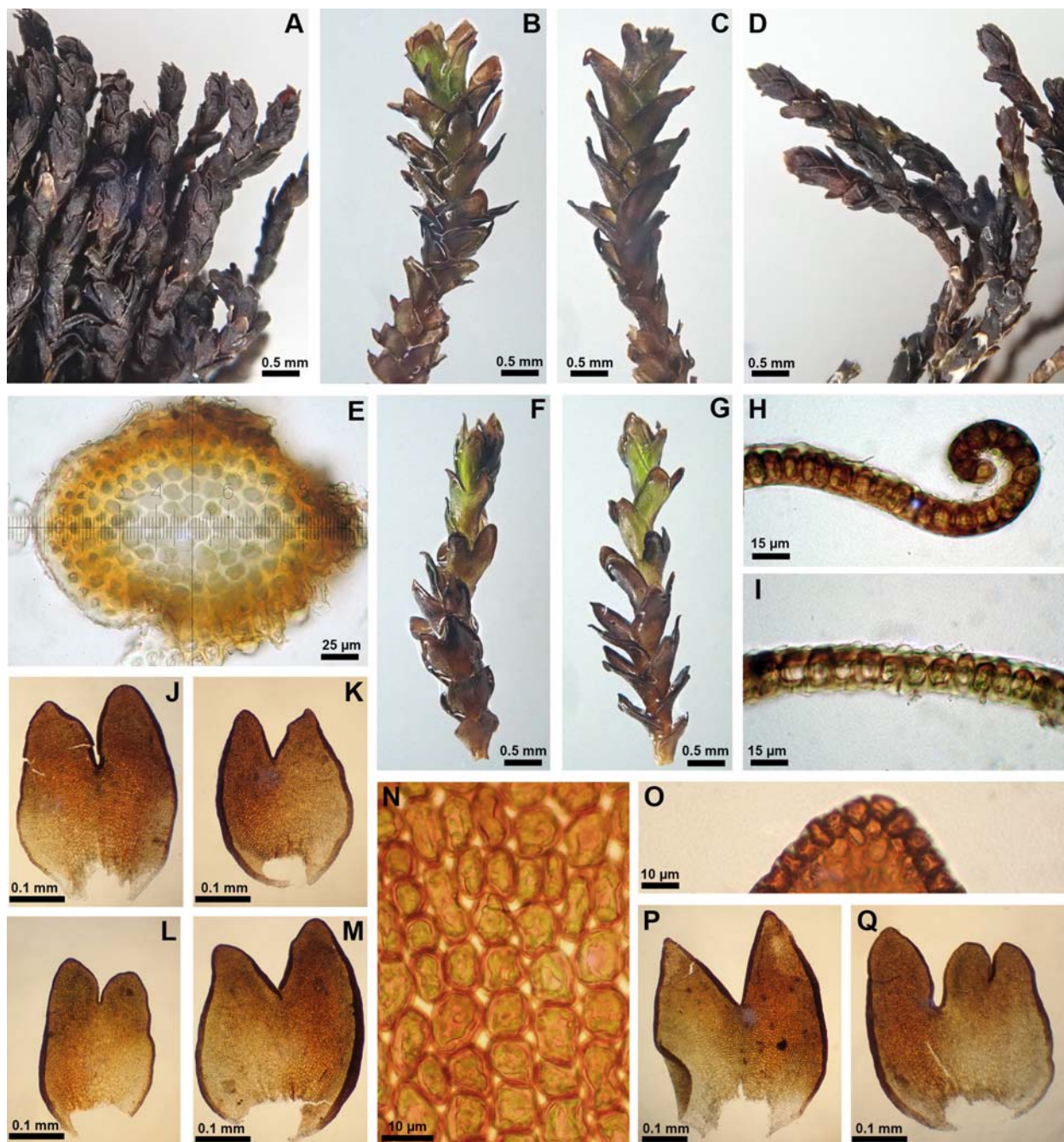


Fig. 6. *Gymnomitrium revolutum* (from Kiebach 3064). A, D: habit, dry; B, C, F, G: habit, moistened; E: stem cross section; H, I: parts of leaf cross sections; J, K, L, M, P, Q: leaves; N: mid-leaf cells; O: leaf lobe apex.

of genetic divergence in nuclear and chloroplast markers suggested all European specimens as *G. revolutum* and specimen *B. Shaw 5764* from China as new to science species, *G. blankae*.

#### TAXONOMY

*Gymnomitrium blankae* Mamontov, Potemkin & Vilnet, sp. nov., Figs. 2–5.

**Diagnosis.** Cinnamon to rusty plants, with leaves somewhat turned dorsally, contiguous to loosely imbricate, bilobed for 0.34–0.47 of their length, with margins rolled backwards through the whole length, with longer

ventral lobes, with apiculate lobes bearing rolled apiculi, with long bleached dorsal and ventral decurrencies; the leaf and stem surfaces smooth; the stem in transverse section with  $\pm$  thinned outer walls of flattened outer cortical cells forming indistinct hyalodermis.

Type: China, Yunnan, Luquan Co., Jiaozixueshan Mtn., ca. 115 km N of Kunming, between lower and middle chair lift station, 26°05'04"N, 102°50'45"E, 3670 m a.s.l., 25.IX.2006, *Blanka Shaw 5764*, det. by J. Váňa as *Marsupella revoluta* (DUKE-180581 – holotype, LE B-0026804 – isotype).



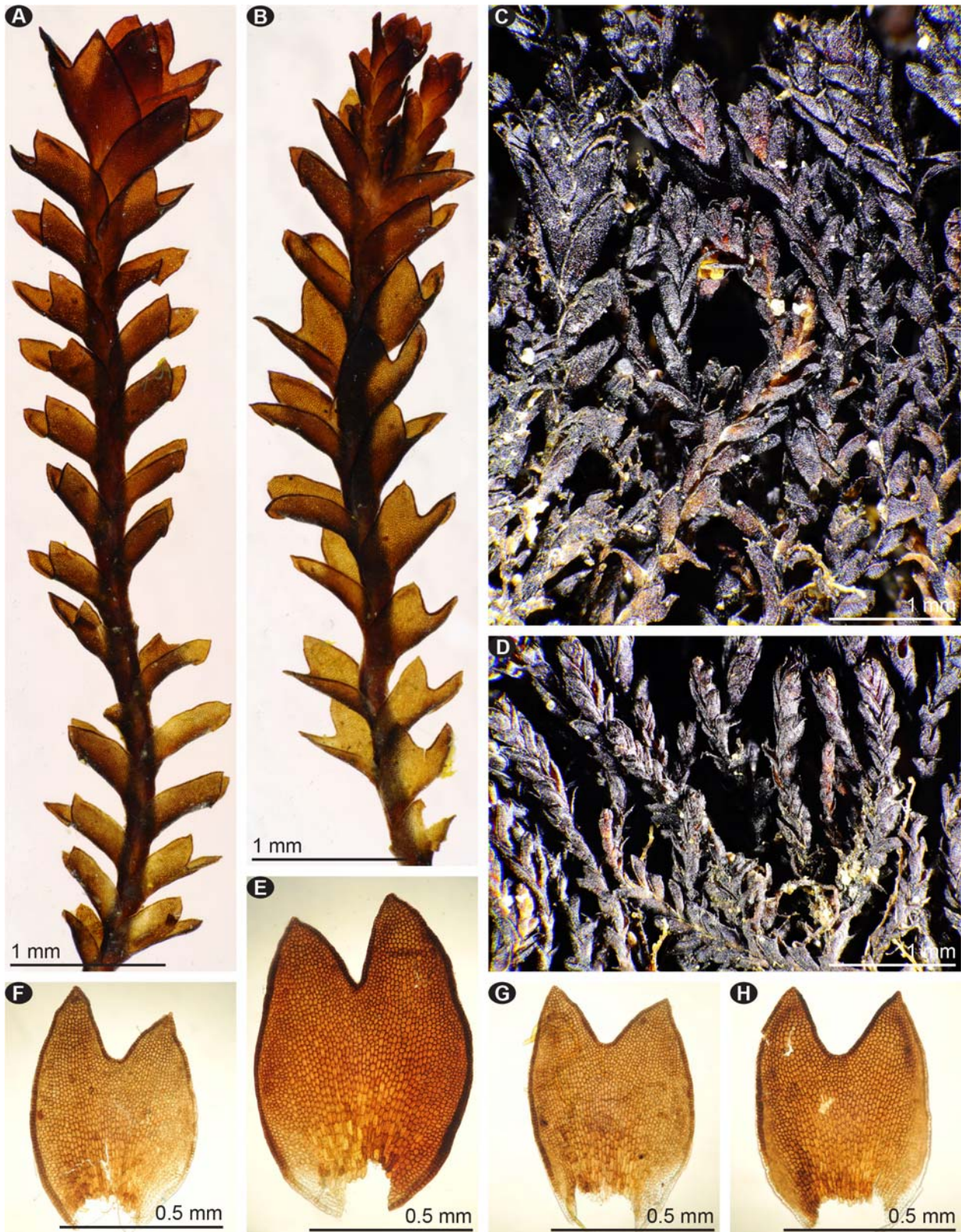


Fig. 7. *Gymnomitrium revolutum* (from Hep. Exs. Lindb., No. 361, MHA). A, B: habit, moistened; C, D: habit, dry; E–H: leaves.

**Etymology.** The species is named after its collector Dr. Blanka Aguero (when collecting Blanka Shaw).

**Description.** Plants ca. 15–20 mm long  $\times$  0.7–1.5 mm wide when wet, 0.2–0.4 mm wide when dry; cinnamon

to rusty when wet (Fig. 3: A–D), darker rusty to fuscous brown when dry (Fig. 2: A–F), with no traces of red pigments, with contiguous to loosely imbricate leaves. Branching rare, lateral intercalary, from upper part of



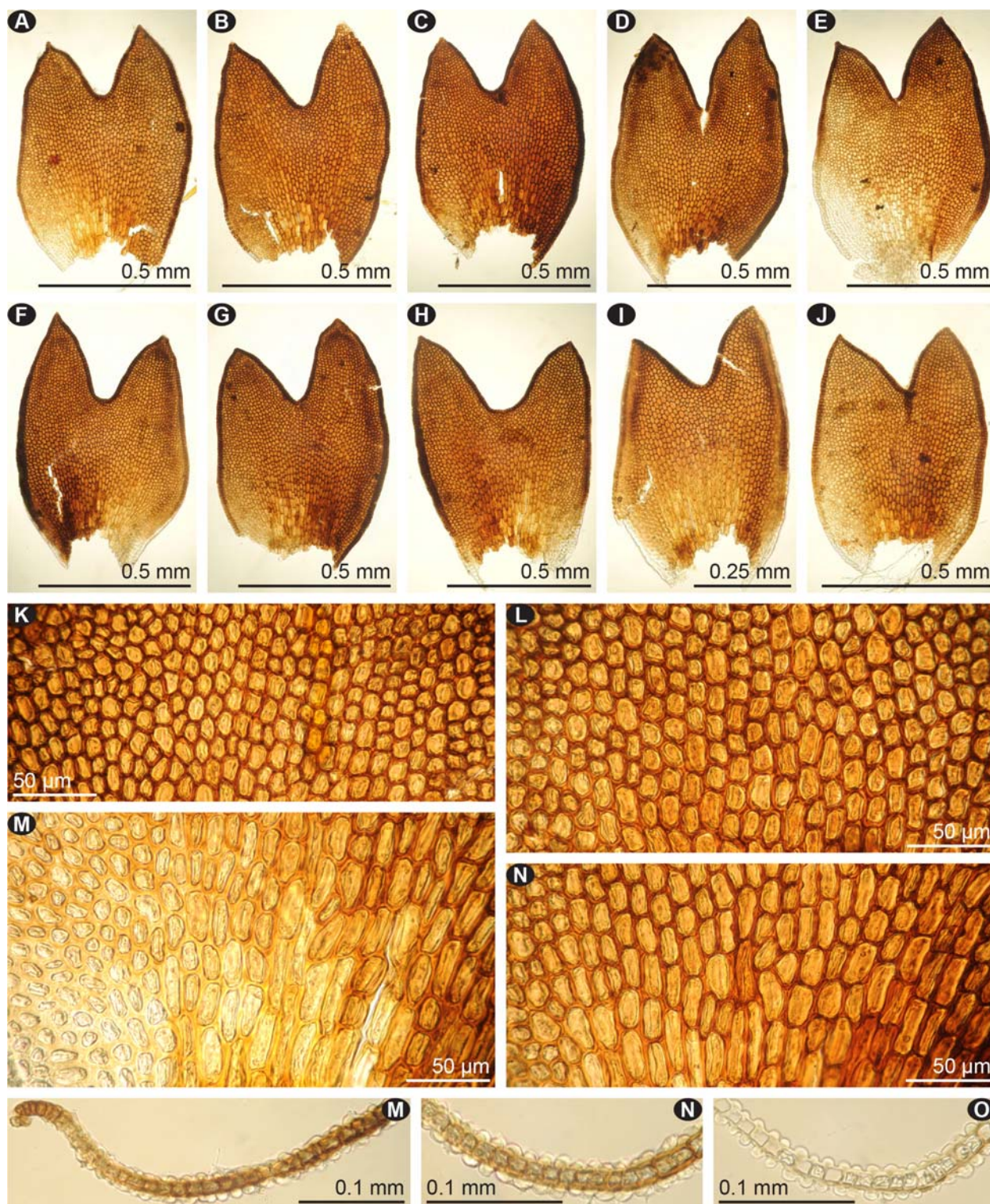


Fig. 8. *Gymnomitrium revolutum* (Nees) H. Philib. (from Hep. Exs. Lindb., No. 361, MHA). A–J: leaves; K: cells of the leaf base near margin; L: basal leaf cells; M–O: parts of leaf cross sections.

the leaf axil in older shoot sectors. Rhizoids lacking or single ones. Stem rigid, in transverse section ca.  $450\ \mu\text{m}$  wide  $\times$   $370\ \mu\text{m}$  high, with 4–5-stratose cortex of 3–4 layers of yellow to brown, rounded strongly thick-walled intracortical cells, and yellowish to nearly colorless, flattened along the stem surface outer cortical cells with thin-

ner but  $\pm$  thickened walls with smooth surface forming  $\pm$  distinct hyalodermis. Leaves contiguous to loosely imbricate, clearly directed to the dorsal side, oblique broadly oval to ovate, with stronger convex ventral margins, longer than wide, ca.  $0.9\text{--}1.2\ \text{mm}$  long  $\times$   $0.7\text{--}0.8\ \text{mm}$  wide, subtransversely inserted, distinctly long decurrent



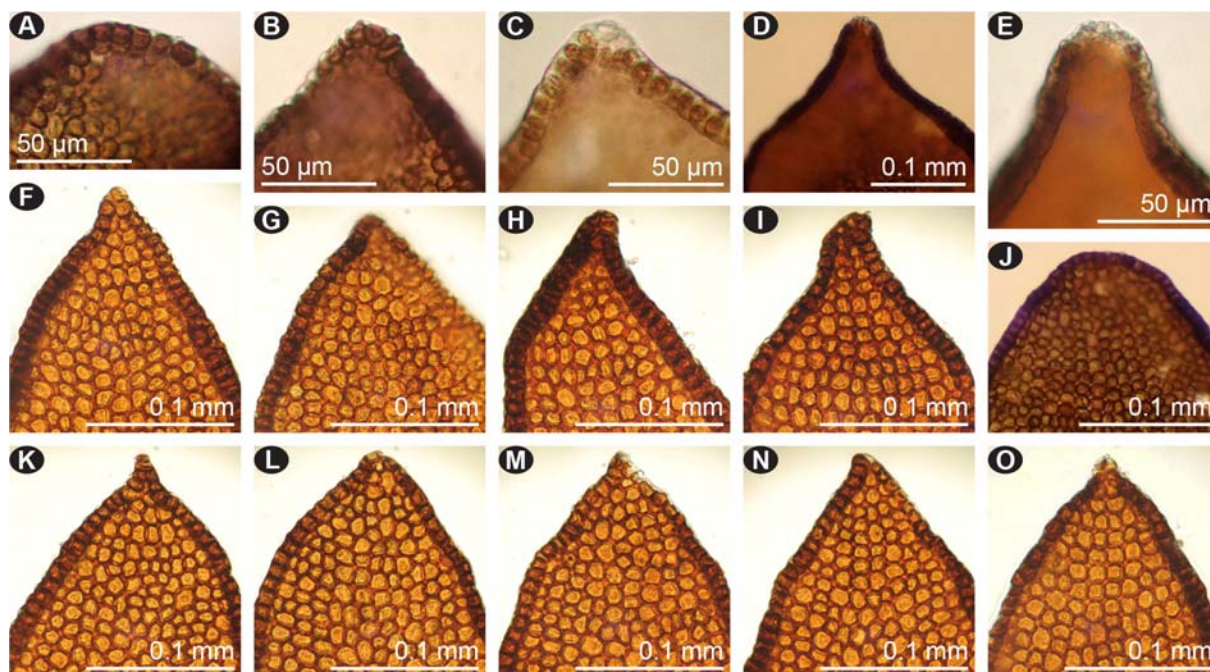


Fig. 9. *Gymnomitrium revolutum* (Nees) H. Philib. (A–E, J from Kiebach 3064, LE B-0026402; F–I, K–O from Hep. Exs. Lindb., No. 361, MHA). A–O: leaf lobe apices.

both dorsally and ventrally (Fig. 5: A–D), with bleached decurrent strips, bilobed; lobes ovate to triangular, usually apiculate with rolled apices (Figs. 3: I, 4: O–S), unequal with always longer ventral lobes; sinus  $\gamma$ - or v-like (0.27–)0.34–0.47 of the leaf length, often somewhat reflexed; undivided part of leaves convex medially, becoming plane to the margins; the margins rolled backwards throughout, i. e., from lobe apices to the decurrent strips and the base of the sinus; width of rolled backwards part from 1 to 6 cells, in distal and proximal parts of leaves narrower, 1–3 cells wide, and in median part of older leaves broader, up to 6 cells wide. Leaf areolation different in proximal and distal parts of leaves. Cells near the base longer and broader, occasionally partly extending to median part of leaves,  $10\text{--}15 \times 20\text{--}40 \mu\text{m}$ , thick-walled with small to larger bulging trigones, usually yellowish. Median and distal cells mostly subisodiametric, with thin wall and rectangular and quadrangular angular thickenings with convex walls, ca.  $10 \mu\text{m}$ , rusty brown. Marginal cells subisodiametric, similar to marginal cells, smaller,  $5\text{--}8 \mu\text{m}$  in diam. or elongated perpendicular to the margin,  $8\text{--}10 \times 5\text{--}7 \mu\text{m}$ , mostly thin-walled or thick-walled because of confluent angular thickenings. Leaf surface smooth. Dioicous. Androecia intercalary, slightly distinct from the sterile shoot sectors. Bracts in 2–3 pairs, similar to sterile leaves, with hardly to moderately convex bases, 2–4- androus. Antheridia on long 2-seriate stalks. Paraphyses lacking. Female plants not seen.

**Distribution and Ecology.** Yunnan, China. Known from the type locality only, where it was collected on vertical base-rich stone face, little shaded in open *Abies-Rhododendron* mixed forest on W-facing steep wet rocky slope.

**Differentiation.** *Gymnomitrium blankae*, being similar to European *G. revolutum* (Figs. 6–8), is distinct in lighter and not characteristic of *G. revolutum* cinnamon to rusty color, Fig. 2: A–D (vs. fuscous, blackish or olive fuscous, Figs. 6: A–D, F, G, 7: A–D); leaves with sinus often  $\gamma$ -like and  $\pm$  reflexed, Figs. 2: G–L, 4: F–L vs. sinus usually V- or U-like not or slightly reflexed, Figs. 6: J–M, P, Q, 7: F–H; apiculate and rolled lobe apices, Figs. 3: I, 4: O–S (vs. rounded to blunt to shortly acute, not or slightly rolled, Figs. 6: 0, 9: A–O); leaf surface smooth in transverse sections, Figs. 3: J–L, 5: I–N and angular thickenings not glistening, Fig. 4: M, N (vs. leaf surface bearing dome-shaped projections above the cell wall intersections, Figs. 6: H, I, 8: M–O, making angular thickenings locally glistening, Fig. 6: N); stem with  $\pm$  thinned outer walls of flattened outer cortical cells forming the indistinct hyalodermis, Fig. 3: G, H (vs. with thickened outer walls of often not flattened outer cortical cells, not forming hyalodermis, Fig. 6: E); base-rich (vs. acidic) habitat; the Sino-Himalayan vs. European distribution.

Noteworthy that leaves of *Gymnomitrium blankae* often have coarser trigones (Fig. 4: M) and smooth surface whereas leaves of *G. revolutum* in general have smaller trigones (Fig. 6: N) and papillose surface. Moreover, leaves of dry shoots of *G. blankae* are usually distinctly turned to the dorsal side of stem, whereas leaves of dry shoots of *G. revolutum* are less often turned to the dorsal side of the stem.

#### DISCUSSION

Study of specimens from the Tyrolean Alps and Norway has shown considerable variability of *G. revolutum*, which was not described and illustrated in previous treat-

ments. It is noteworthy that European plants often develop leaves with somewhat longer ventral lobes and sometimes with deeper sinuses, up to 0.45 the leaf length. However, the lobes are often obtuse to rounded, rarely with rolled vestigial apiculi resembling those of *G. blankae*. Worth mentioning that in previous illustrations of European *Gymnomitrium revolutum* (Müller, 1956: Fig. 264; Damsholt, 2002: Plate 103) leaves have nearly subequal lobes, occasionally with plane margins (Damsholt, 2002: Plate 103: 5). In studied by us Norwegian plants, sinus shallower than in the plants from the type locality and margins less enrolled than in the plants from the type locality (Fig. 7: F–H vs. Fig. 6: J–M, P, Q, respectively).

Concerning the leaf surface ornamentation Schuster (2002) noted that ‘in typical subsp. *revoluta* [*G. revolutum* subsp. *revolutum* – auth. note] the cuticle is clearly verrucose’ (l.c., p. 560), ‘although some Arctic populations of subsp. *revoluta* may have the cuticle seemingly “smooth” (Schuster 1974)’ (l.c., p. 562). The studied here shoots from the Tyrolean Alps reveal low indistinct projections above the trigones of leaf cells (Fig. 6: H, I). In the Norwegian plants, the projections above the cell walls intersections are more or less high and hemispherical (Fig. 8: M–O), although poorly visible due to high transparency. In the upper half of leaves, they are rounded to elliptical (in view from above), large and merged, broadened to cover the surface over cell walls between trigones, whereas in the lower part of leaves they are merged in bands covering the cell walls and trigones. These projections possibly result in glistening surface of the dried shoots of the Norwegian plants of *G. revolutum* (Fig. 7: C, D). By the presence of dome-like projections on leaf surfaces, *G. revolutum* is similar to the remotely allied taxa *G. parvitextum* (Steph.) Mamontov et al. and *G. verrucosum* W.E. Nicholson, while the species phylogenetically most closely related to *G. revolutum*, namely *G. africanum* and *G. sichuanicum* Bakalin & Vilnet, as well as the newly described *G. blankae*, have smooth leaf surface. Several other species, such as *G. commutatum* (Limpr.) Schiffn., *G. crystallocaulon* (Grolle) Váňa et al., *G. fissum*, *G. rubidum* (Mitt.) Váňa et al., and *G. schusterianum*, which are not closely related to *G. revolutum* and *G. blankae*, also have smooth leaf surface. Therefore, the presence or absence of dome-shaped projections on the leaf surface may be important, as suggested by Schuster (2002: 562), in the taxonomy of the *Gymnomitrium revolutum* complex or the former *Apomarsupella*-group. For morphological differentiation of these species, the structure of leaf surface should be analyzed together with cuticular ornamentation of stem, the shape and orientation of leaves, the shape of leaf lobe apices, the depth of leaf sinus, as well as the degree of development of revolute leaf margins and the leaf vitta.

#### CONCLUSION

This study led us to confirm previously stated conclusions on “the expediency of considering the “geo-

graphical races” of widespread species as independent taxa and the wide distribution of convergence in bryophyte evolution” and on the increasing number of new species in the very near future (Potemkin *et al.*, 2021). Our morphological study of specimens from Europe and Asia, identified as *Gymnomitrium revolutum* ( $\equiv$  *Marsupella revoluta*), demonstrates their considerable distinctions and demands their further morphological and molecular investigation.

#### ACKNOWLEDGMENTS

This study became possible due to material of *Gymnomitrium revolutum* from the type locality send us by T. Kiebachner and H. Köckinger, whose help is greatly appreciated. Our cordial thanks are due to Edwin Urmi for his kind arrangements for this study, and to Yuri Okolodkov and Marcia Gowing for careful reading the text and correcting the English. The authors are deeply grateful to Dr. Blanka Aguero (DUKE) for lending the *Gymnomitrium* collections from Yunnan Province, China for morphological studies and for permission to keep in LE the part of the specimen *B. Shaw 3064*, which published here as isotype of *G. blankae*. Help of Mrs. Lyudmila A. Kartseva in SEM study is gratefully appreciated. The research was done using equipment of The Core Facility Center «Cell and Molecular Technologies in Plant Science» at the Komarov Botanical Institute RAS (St. Petersburg, Russia). The study of A.D. Potemkin was financially supported by the Ministry of Science and Higher Education of the Russian Federation under Agreement No. 075-15-2021-1056, the study of Yu.S. Mamontov was financially supported by the Ministry of Science and Higher Education of the Russian Federation under Agreement No. 075-15-2021-678 for supporting Center of Common Use «Herbarium MBG RAS».

#### LITERATURE CITED

- BAKALIN, V., A. VILNET, D. LONG, K. KLIMOVA, YU. MALTSEVA, V.S. NGUYEN & W.Z. MA. 2022. On two species of *Gymnomitrium* (Gymnomitriaceae, Marchantiophyta) in the Eastern Sino-Himalaya. – *Phytotaxa* **533** (2): 117–136. <https://doi.org/10.11646/phytotaxa.533.2.1>
- BUCH, H. 1928. Die Scapanien Nordeuropas und Sibiriens 2. Systematischer Teil. Soc. Sci. Fenn. Comm. Biol. **3**(1): 1–177.
- DAMSHOLT, K. 2002. Illustrated flora of Nordic liverworts and hornworts. Nordic Bryol. Soc., Lund: 840 p.
- HALL, T.A. 1999. BioEdit: a user-friendly biological sequence alignment editor and analysis program for Windows 95/98/NT. – *Nucleic Acids Symposium Series* **41**: 95–98.
- HOANG, D.T., O. CHERNOMOR, A. VON HAESELER, B.Q. MINH & L.S. VINH. 2018. UFBoot2: Improving the ultrafast bootstrap approximation. – *Molecular Biology and Evolution* **35**(2): 518–522. <https://doi.org/10.1093/molbev/msx281>
- KALYAANAMOORTHY S., B.Q. MINH, T.K.F. WONG, A. VON HAESELER & L.S. JERMIIN. 2017. ModelFinder: Fast model selection for accurate phylogenetic estimates. – *Nature Methods*. **14**: 587–589. <https://doi.org/10.1038/nmeth.4285>
- KONSTANTINOVA, N.A., D.G. LONG, YU.S. MAMONTOV & A.A. VILNET. 2021. *Gymnomitrium schusterianum* (Gymnomitriaceae), a new species from the Sino-Himalaya. – *Arctoa* **30**: 149–158. <https://doi.org/10.15298/arctoa.30.16>



- MAMONTOV, YU.S., N.A. KONSTANTINOVA, A.A. VILNET, A.D. POTEKIN, E.V. SOFRONOVA & N.S. GAMOVA. 2018. On resurrection of *Marsupella parvitexta* Steph. (Gymnomitriaceae, Marchantiophyta) as a semi cryptic species of the genus *Gymnomitrium*. – *Nova Hedwigia* **106** (1–2): 81–101. [https://doi.org/10.1127/nova\\_hedwigia/2017/0466](https://doi.org/10.1127/nova_hedwigia/2017/0466)
- MAMONTOV, YU.S., A.A. VILNET, N.A. KONSTANTINOVA & V.A. BAKALIN. 2019. Two new species of Gymnomitriaceae (Marchantiophyta) in the North Pacific. – *Botanica Pacifica* **8**(1): 67–80. <https://doi.org/10.17581/bp.2019.08113>
- MÜLLER, K. 1956. Die Lebermoose Europas (Musci hepatici). In: L. Rabenhorst's Kryptogamen-Flora von Deutschland, Österreich und der Schweiz. Bd VI, 3 Aufl., Lief. 6. Leipzig, S. 757–916.
- NEES, C.G. 1836. Naturgeschichte der Europäischen Lebermoose, vol. 2. August Rücker, Berlin, 499 pp.
- NGUYEN L.-T., H.A. SCHMIDT, A. VON HAESELER & B.Q. MINH. 2015. IQ-TREE: A fast and effective stochastic algorithm for estimating maximum likelihood phylogenies. – *Molecular Biology and Evolution* **32** (1): 268–274. <https://doi.org/10.1093/molbev/msu300>
- POTEKIN, A.D., YU.S. MAMONTOV & N.S. GAMOVA. 2017. *Gymnomitrium fissum* (Gymnomitriaceae, Marchantiophyta) – a new species with fissured leaf surface from China. – *Novosti sistematiki nizshikh rastenii* **51**: 274–280. <https://doi.org/10.31111/nsnr/2017.51.274>
- POTEKIN, A., V. BAKALIN, A. VILNET, K. KLIMOVA & E. KUZMINA. 2021. A survey of the section *Scapania* of the genus *Scapania* (Scapaniaceae) with description of new species *Scapania pseudouliginosa* and resurrection of *S. gigantea*. – *The Bryologist* **124**(4): 569–589. <https://doi.org/10.1639/0007-2745-124.4.569>
- RONQUIST, F., M. TESLENKO, P. VAN DER MARK, D.L. AYRES, A. DARLING, S. HÖHNA, B. LARGET, L. LIU, M.A. SUCHARD & J.P. HÜLSENBECK. 2012. MrBayes 3.2: Efficient Bayesian phylogenetic inference and model choice across a large model space. – *Systematic Biology* **61**: 539–542.
- SHAW, B., B. CRANDALL-STOTLER, J. VÁÑA, R.E. STOTLER, M. VON KONRAT, J.J. ENGEL, E.C. DAVIS, D.G. LONG, P. SOVA & A.J. SHAW. 2015. Phylogenetic Relationships and Morphological Evolution in a Major Clade of Leafy Liverworts (Phylum Marchantiophyta, Order Jungermanniales): Suborder Jungermanniineae. – *Systematic Botany*, **40**(1): 27–45. <https://doi.org/10.1600/036364415X686314>
- SÖDERSTRÖM, L., A. HAGBORG, M. VON KONRAD, S. BARTHOLOMEW-BEGAN, D. BELL, L. BRISCOE, E. BROWN, D.C. CARGILL, D.P. COSTA, B.J. CRANDALL-STOTLER, E.D. COOPER, G. DAUPHIN, J.J. ENGEL, K. FELDBERG, D. GLENNY, S.R. GRADSTEIN, X. HE, J. HEINRICHS, J. HENTSCHER, A.L. ILKIUBORGES, T. KATAGIRI, N.A. KONSTANTINOVA, J. LARRAÍN, D.G. LONG, M. NEBEL, T. PÓCS, F. FELISA PUCHE, E. REINER-DREHWALD, M.A.M. RENNER, A. SASS-GYARMATI, A. SCHÄFER-VERWIMP, J.G.S. MORAGUES, R.E. STOTLER, P. SUKKHARAK, B.M. THIERS, J. URIBE, J. VÁÑA, J.C. VILLARREAL, M. WIGGINTON, L. ZHANG & R.-L. ZHU. 2015. World checklist of hornworts and liverworts. – *PhytoKeys* **59**: 1–828. <https://doi.org/10.3897/phytokeys.59.6261>
- TAMURA, K., G. STECHER & S. KUMAR. 2021. MEGA11: Molecular Evolutionary Genetics Analysis version 11. – *Molecular Biology and Evolution* **38**: 3022–3027. <https://doi.org/10.1093/molbev/msab120>
- TABERLET, P., L. GIELLY, G. PAUTOU & J. BOUVET. 1991. Universal primers for amplification of three non-coding regions of chloroplast DNA. – *Plant Molecular Biology* **17**: 1105–1109.
- WHITE, T.J., T. BRUNS, S. LEE & J. TAYLOR. 1990. Amplification and direct sequencing of fungal ribosomal RNA genes for phylogenetics. In: Innis, M. A., Gelfand, D. H., Snisky, J. J. & White, T. J. (eds.) *PCR protocols: a guide to methods and applications*. San Diego, pp. 315–322.

Appendix 1. The list of molecularly tested specimens with vouchers and GenBank accession numbers, accessions obtained in this study are in bold.

Taxon	Specimen voucher	GenBank accession number	
		ITS1-2 nrDNA	trnL-F cpDNA
<i>Gymnomitrium africanum</i> (Steph.) Horik.	Rwanda, <i>Pocs 8210</i> (F)	no data	KF943101
<i>G. blankae</i> Mamontov, Potemkin & Vilnet sp. nov.	China: Yunnan Province, <i>Shaw 5764</i> (LE B-0026804, DUKE-180581, as <i>G. revolutum</i> (Nees) H. Philib.)	<b>OQ024239</b>	KF943024
<i>G. brevissimum</i> (Dumort.) Warnst.	Russia: Murmansk Region, <i>Konstantinova</i> (KPABG-8171)	EU791833	EU791711
<i>G. commutatum</i> (Limpr.) Schiffn.	Austria: Tyrol, <i>Köckinger 41502, 15048</i> (Herb. Köckinger, KPABG)	MF521468	MF521479
<i>G. concinnatum</i> (Lightf.) Corda	Russia: Republic of Karachaevo-Cherkessia, <i>Konstantinova K465a-05</i> (KPABG-109696)	EU791831	EU791710
<i>G. corallioides</i> Nees	Norway: Svalbard, <i>Konstantinova K155-04</i> (KPABG-110103)	EU791826	EU791705
<i>G. crystallocaulon</i> (Grolle) Váňa et al.	China: Yunnan Province, <i>Long &amp; Shevock 37244</i> (MO)	MH826403	MH822628
<i>G. fissum</i> Mamontov & Potemkin	China: Yunnan Province, <i>Long 34872</i> (MO)	MH826404	MH822629
<i>G. kamchaticum</i> Mamontov et al.	Russia: Kamchatka Territory, <i>Bakalin K-44-19-15</i> (VBGI, KPABG, MHA)	MH826407	MH822631
<i>G. mucronulatum</i> (N. Kitag.) N. Kitag.	Japan, <i>Bakalin J-86-5-15</i> (VBGI)	MK084619	MK073904
<i>G. obtusum</i> Lindb.	Finland, <i>Parnela H-4224851</i> (duplicate in KPABG)	MH826406	MH822630
<i>G. pacificum</i> Grolle	Russia: Kamchatka Territory, <i>Bering I., Bakalin K-26-4-02-VB</i> (KPABG-103350)	EU791835	EU791713
<i>G. parvitextum</i> (Steph.) Mamontov et al.	Russia: Primorye Territory, <i>Mamontov 170-1-10</i> (KPABG)	MF521472	MF521482
<i>G. revolutum</i> (Nees) H. Philib.	Austria, <i>H. Köckinger #15427</i> (LE B-00264401)	<b>OQ024237</b>	<b>OQ029673</b>
<i>G. revolutum</i>	Italy, <i>Kiebachner 3064</i> (LE B-00264402)	<b>OP806305</b>	<b>OP821980</b>
<i>G. revolutum</i>	Switzerland, <i>T. Kiebachner #2235</i> (LE B-0026405)	<b>OQ024235</b>	<b>OQ029671</b>
<i>G. revolutum</i>	Switzerland, <i>T. Kiebachner #2375</i> (LE B-0026406)	<b>OQ024236</b>	<b>OQ029672</b>
<i>G. rubidum</i> (Mitt.) Váňa et al. subsp. <i>rubidum</i>	China: Yunnan Province, <i>Bakalin C-72-17-18</i> (VBGI, KPABG-125501)	MW381014	MW387158
<i>G. rubidum</i> subsp. <i>subvittatum</i> Vilnet et al.	China: Yunnan Province, <i>Long 34462</i> (DUKE, KPABG-123703)	MW822010	MW841071/KF943103
<i>G. sichuanicum</i> Bakalin & Vilnet	China: Sichuan Province, <i>Bakalin &amp; Klimova China-43-1-17</i> (VBGI, KPABG)	MK084621	MK073906
<i>G. schusterianum</i> Konstant. et al.	China: Yunnan Province, <i>Long 35728</i> (MO, duplicate in KPABG, MHA)	OK493146	OK482715
<i>Gymnomitrium</i> sp.	China: Yunnan Prov., <i>J. Shevock #23313</i> (MO)	<b>OQ024238</b>	<b>OQ029674</b>
<i>Gymnomitrium</i> sp. det. as “ <i>revolutum</i> ”	Russia: Trans-Baikal Territory, <i>Mamontov, Bryoph. Ross. Civ. Coll. Exs. Fasc. XI, No. 453</i> (KPABG-121724)	OK493148	<b>OP821981</b>
<i>G. verrucosum</i> W.E. Nicholson	China: Yunnan Province, <i>Long &amp; Shevock 37182</i> (DUKE)	no data	KJ802102
<i>Prasanthus suecicus</i> (Gottsche) Lindb.	Norway: Svalbard, <i>Konstantinova K 121-5-06</i> (KPABG)	EU791825	EU791704

Received 20 October 2022

Accepted 16 December 2022